

Like-sign muon-electron production by neutrinos: Key to trilepton mechanisms*

V. Barger, T. Gottschalk, D. V. Nanopoulos, and R. J. N. Phillips[†]

University of Wisconsin, Physics Department, Madison, Wisconsin 53706

(Received 18 July 1977; revised manuscript received 26 September 1977)

The most promising explanations of $\nu N \rightarrow \mu^- \mu^- X$ and $\nu N \rightarrow \mu^- e^- X$ like-sign dilepton events are two classes of models that have recently been proposed to explain neutrino trimuon production: (i) cascade decay of a charged heavy lepton M^- , (ii) decay of a neutral heavy lepton M^0 together with semileptonic decay of a new quark b . These two classes predict quite different lepton energies for $\nu N \rightarrow \mu^- e^- X$ events. They also predict completely different charge topologies for antineutrino-produced trileptons and like-sign dileptons.

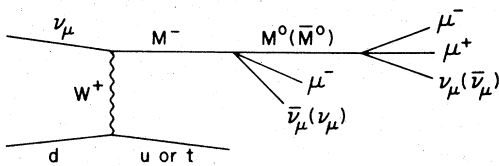
Two radically different classes of heavy-lepton mechanisms have been proposed to explain the neutrino production of trimuons^{1,2}: (i) cascade decays $M^- \rightarrow M^0 \mu^- \bar{\nu}$ (or $\nu \mu^- M^0 \rightarrow \mu^- \mu^- \mu^+ \nu \bar{\nu}$) of a heavy lepton M^- produced along with old or new hadrons³⁻⁹; (ii) lepton-hadron mechanisms^{5,8,10} where a heavy lepton M^0 is produced via a neutral current along with a new quark b of charge $-\frac{1}{3}$, followed by the decays $M^0 \rightarrow \mu^- \mu^+ \nu$ and $b \rightarrow u \mu^- \bar{\nu}$ (see Fig.1). It seems difficult to discriminate between these two classes on the basis of rather few trimuon events, now or in the near future. However, both classes of mechanisms predict other interesting phenomena. Of particular interest are like-sign dilepton events¹¹ and also antineutrino production of trileptons and dileptons. In this paper we show that the lepton energies in $\nu N \rightarrow \mu^- e^- X$ events distinguish clearly between these two classes of mechanisms. We also show that the predicted charge topologies for antineutrino-produced trileptons and dileptons are completely different for the two classes.

The trimuon mechanisms generally predict νN

$\rightarrow \mu^- \mu^- X$ events at a few times the trimuon rate, from diagrams where M^0 decays hadronically, $M^0 \rightarrow \mu^- H^+$, and from $M^0 \rightarrow \mu^- l^+ \nu$ when the lepton l^+ is not identified experimentally. (Exceptions to this are models^{6,10} where the hadron system H^+ has to contain a heavy quark; here the $\mu^- \mu^-$ rate is much reduced and may well be too low to fit experiment.¹²) Cascade decays via \bar{M}^0 do not give pure $\mu^- \mu^-$ events since μ^+ is present too, but models with \bar{M}^0 modes also have cascades via M^0 . Likewise, $\nu N \rightarrow \mu^- e^- X$ events are predicted at a rate similar to $\mu^- \mu^-$ (see Fig. 2).

Our crucial observation about $\mu^- e^-$ events is that the e^- comes from quite different places in the lepton-cascade and lepton-hadron pictures, so that its properties can be used to discriminate sensitively between these alternatives. This is true of $\mu^- \mu^-$ events also, but to a lesser extent since information about the matrix element is lost here through the indistinguishability of the muons. Both $\mu^- \mu^-$ and $\mu^- e^-$ events have been reported^{12,13}; confirmation of such like-sign dilepton events is an essential test of trimuon mechanisms.

LEPTON-CASCADE TRIMUON MECHANISM



LEPTON-HADRON TRIMUON MECHANISM

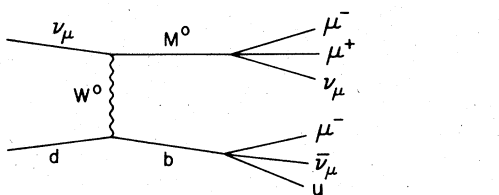
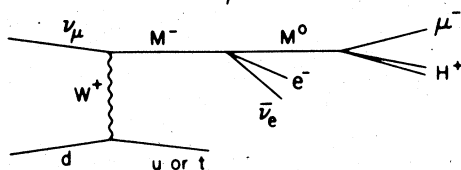


FIG. 1. Dominant diagrams for $\nu N \rightarrow \mu^- \mu^- \mu^+ X$ trimuon production in lepton-cascade and lepton-hadron models.

LEPTON-CASCADE $\mu^- e^-$ MECHANISM



LEPTON-HADRON $\mu^- e^-$ MECHANISM

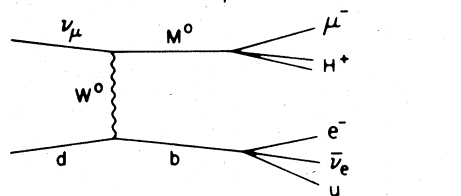


FIG. 2. Dominant diagrams for $\nu N \rightarrow \mu^- e^- X$ like-sign dilepton production in lepton-cascade and lepton-hadron models.

The following simple qualitative argument illustrates the difference between the two classes of μ^-e^- production mechanism. For $V-A$ coupling at the quark vertex, the incident neutrino energy E is equally shared on average between the primary heavy lepton and the produced quark. In M^0 decay, the M^0 energy is distributed roughly equally on average among the three decay particles (leptons or light quarks). In $M^- \rightarrow M^0 e^- \bar{\nu}$ decay, however, M^0 takes a larger fraction of the M energy—approximately one half in fact³—because of its larger mass, while e and ν take about one quarter each. In heavy-quark fragmentation with fragmentation function $D(z) \propto e^{-\beta z}$, the new meson carries mean energy fraction

$$\langle E(\text{meson}) \rangle / \langle E(\text{quark}) \rangle = \beta^{-1} - (\beta^{\beta} - 1)^{-1} \quad (1)$$

asymptotically. The value $\beta \approx 3$ is indicated¹⁴ by charm fragmentation data from Fermilab.^{12,13} Assuming a similar dependence for heavier quarks, the new meson carries about one third of the b -quark energy on average, of which it distributes approximately one third to each decay lepton. Hence we obtain the qualitative predictions for μ^-e^- events

$$\langle E_{\mu} \rangle \approx \frac{2}{3} \langle E_e \rangle \approx \frac{1}{12} E, \quad \text{lepton-cascade models,} \\ V-A \text{ quarks} \quad (2)$$

$$\langle E_{\mu} \rangle \approx 3 \langle E_e \rangle \approx \frac{1}{6} E, \quad \text{lepton-hadron models,} \\ V-A \text{ quarks.} \quad (3)$$

For $V+A$ coupling at the quark vertex, the final quark takes one quarter of the neutrino energy on average, and the model differences become more pronounced:

$$\langle E_{\mu} \rangle \approx \frac{2}{3} \langle E_e \rangle \approx \frac{1}{8} E, \quad \text{lepton-cascade models,} \\ V+A \text{ quarks} \quad (4)$$

$$\langle E_{\mu} \rangle \approx 9 \langle E_e \rangle \approx \frac{1}{4} E, \quad \text{lepton-hadron models,} \\ V+A \text{ quarks.} \quad (5)$$

These estimates are only qualitative, and incorporate asymptotic approximations, but they

show some of the trends. If the fragmentation function is concentrated at higher z than assumed above, as seems to be indicated by an analysis¹⁵ of recent CERN charm fragmentation data,¹⁶ or as may be the case for the b quark, the distinctions between lepton-cascade and lepton-hadron model predictions are not as dramatic but similar qualitative differences persist, as documented later.

To put these estimates on a firmer basis, we have made realistic calculations of some typical cases, with properties as listed in Table I.

We calculate the heavy-lepton-cascade mechanism by the methods described in Ref. 3. For model LC3 with new-quark production, we add slow rescaling as described in Ref. 17. In the decay $M^0 \rightarrow \mu^- H^+$, the hadron system is represented by light quarks with $V-A$ coupling.

We calculate the M^0 production and decay in LH models from standard formulas¹⁸ modified to include heavy-quark production with slow rescaling. The heavy-quark-to-heavy-meson transition is described by a fragmentation function $D(z) \sim e^{-3z}$ following the results for charm fragmentation found in Ref. 14. The heavy-meson decay is described by a spin-0 three-body-decay matrix element, with a heavy-meson mass equal to the b -quark mass and a massless decay hadron; this prescription is conservative, in that it maximizes the energy fed into the decay e^- and minimizes the difference between LH and LC models.

The characteristic dynamical differences between LC and LH models show up most clearly in a scatter plot of $E(\mu^-)$ versus $E(e^-)$. A big advantage of energy scatter plots is that any experimental energy acceptance cuts can be superimposed. The results for all LC models are qualitatively very similar: The results for all LH models resemble each other closely, too, but LC and LH classes differ markedly from each other. Figure 3 illustrates one typical case from each class, models LC1 and LH1, averaged over the neutrino spectrum of the BNL-Columbia experiment.¹³ The dashed lines in Fig. 3 outline a 99% boundary of LH-class scatter plots. Note that LC models pop-

TABLE I. Properties of models used in calculations. The labels LC and LH refer to lepton-cascade and lepton-hadron models, respectively. Particle masses are in GeV.

Model	M^- mass	M^0 mass	New-quark mass	$M^- \rightarrow M^0$ coupling	$M^0 \rightarrow \mu$ coupling	Quark transitions
LC1	7.0	2.5		L	R	$d \rightarrow u(L)$
LC2	7.0	2.5		R	R	$d \rightarrow u(R)$
LC3	7.0	2.5	4.0	R	R	$d \rightarrow t(R)$
LH1		5.0	5.0		R	$d \rightarrow b(L)$
LH2		5.0	5.0		L	$d \rightarrow b(L)$
LH3		5.0	5.0		R	$d \rightarrow b(R)$

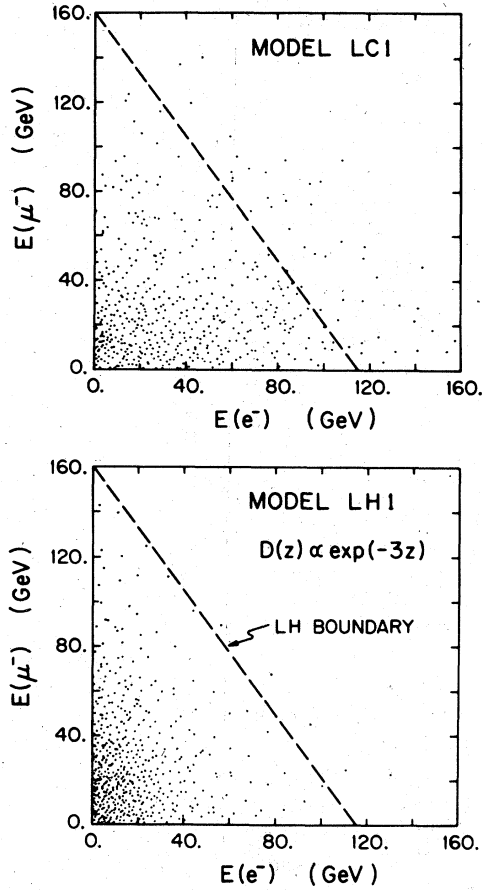


FIG. 3. Scatter plots of $E(\mu^-)$ vs $E(e^-)$ for $\nu N \rightarrow \mu^- e^- X$, averaged over the neutrino spectrum of Ref. 13 for models LC1 and LH1 that are typical of the two classes. A fragmentation function $D(z) \sim e^{-3z}$ is used for the LH1 model. The dashed lines outline a 99% boundary of the LH-class scatter plots.

ulate the region inaccessible to LH models, and also give different density distributions in the allowed region.

Quantitative differences between LC and LH classes also appear in the average μ^- and e^- energies. Calculated values for the spectrum of Ref. 13 are in Table II. To enable comparison

TABLE II. Average energies of μ^- , e^- , and incident neutrino ($\langle E \rangle$) in various models for the spectrum of Ref. 13.

Model	$\langle E(\mu^-) \rangle$ (GeV)	$\langle E(e^-) \rangle$ (GeV)	$\langle E \rangle$ (GeV)	$\langle E(\mu^-) \rangle / \langle E(e^-) \rangle$
LC1	19	35	174	0.55
LC2	24	46	174	0.52
LC3	23	44	203	0.52
LH1	31	14	194	2.3
LH2	36	14	194	2.6
LH3	35	11	194	3.1

TABLE III. Average energies of μ^- , e^- , and incident neutrino ($\langle E \rangle$) in various models with the BNL-Columbia experimental acceptance cuts, $E(\mu^-) > 10$ GeV, $E(e^-) > 1$ GeV.

Model	$\langle E(\mu^-) \rangle$ (GeV)	$\langle E(e^-) \rangle$ (GeV)	$\langle E \rangle$ (GeV)	$\langle E(\mu^-) \rangle / \langle E(e^-) \rangle$
LC1	29	36	185	0.80
LC2	33	46	185	0.73
LC3	31	44	208	0.70
LH1	39	15	198	2.7
LH2	45	15	198	3.1
LH3	44	12	198	3.6

with our qualitative predictions, Eqs. (2)–(5), we also give the calculated mean energy $\langle E \rangle$ of the incident neutrino for each model. These numbers are reasonably consistent with our simplified estimates of Eqs. (2)–(5), and any discrepancies can be understood as threshold effects. When we incorporate the BNL-Columbia experimental acceptance cuts $E(\mu^-) > 10$ GeV, $E(e^-) > 1$ GeV, the corresponding average values are given in Table III. These results indicate that the μ^-/e^- energy ratio in $\nu N \rightarrow \mu^- e^- X$ events distinguishes sharply between the LC and LH classes of mechanisms.

We next analyze the consequences of a harder b -quark fragmentation function by comparing $D(z) \propto e^{-\beta z}$ calculations for the cases $\beta = 3, 0, -3$. For the LH1 model the average energies including acceptance corrections are given in Table IV. Even for the $\beta = -3$ case, the ratio $\langle E(\mu^-) \rangle / \langle E(e^-) \rangle$ is almost a factor of two higher in LH models than in LC models. Figure 4 illustrates LH results in the $E(\mu^-)$ versus $E(e^-)$ scatter plot for the $\beta = 0$ and $\beta = -3$ cases. The 99% LH boundary of Fig. 3 is a 98% boundary for $\beta = 0$ and a 96% boundary for $\beta = -3$. For comparison 90% of LC events would lie within this boundary.

Some qualifying remarks should now be added:

(i) We have excluded $M^- \rightarrow M_0 \mu^- \bar{M}^0$ decays, which can cascade to multilepton states,^{3,5} because they are phase-space suppressed.

(ii) We have ignored M^- decays via a doubly charged⁷ heavy lepton M^{--} , because there is no evidence for such a particle lighter than M^- .

TABLE IV. Average energies (including acceptance corrections) in LH1 model for various b -quark fragmentation functions $D(z) \propto e^{-\beta z}$.

β	$\langle E(\mu^-) \rangle$ (GeV)	$\langle E(e^-) \rangle$ (GeV)	$\langle E(\mu^-) \rangle / \langle E(e^-) \rangle$
3	39	15	2.7
0	39	22	1.8
-3	39	28	1.4

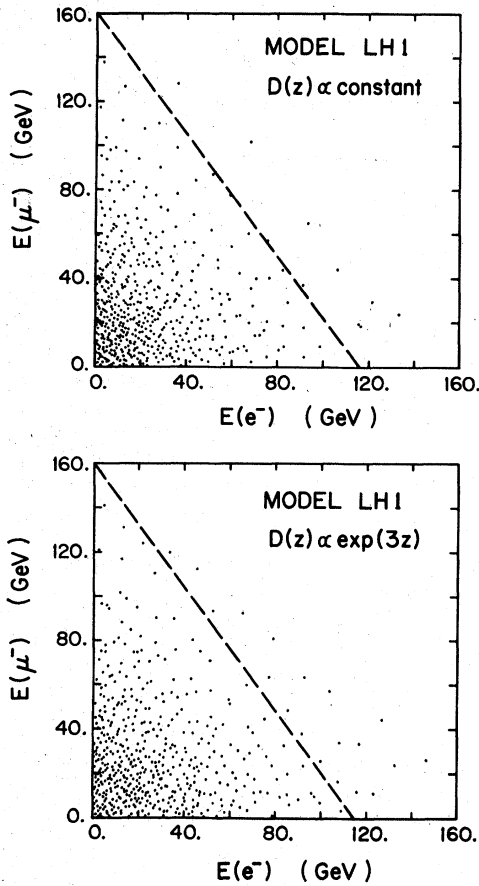


FIG. 4. Scatter plots for model LH1 with fragmentation functions $D(z) \propto \text{constant}$ and $D(z) \propto e^{3z}$. The boundary curve shown is that of Fig. 3.

(iii) Our arguments tacitly assume that muon and electron weak-current sectors are approximately decoupled.

(iv) We have excluded M^0 cascade decays via heavy leptons E^0 of the electron family, which can give the classes of μ^+e^- events shown in Fig. 5, for the following reasons. $M^0 \rightarrow \mu^+E^0e^+$ decays lead to μ^+e^- with an accompanying e^+ , which would be detected with good efficiency in the μe experiments; events with undetected e^+ are suppressed. The other diagram in Fig. 5, giving μ^+e^- events through $E^0 \rightarrow e^-H^+$ and $b \rightarrow u\mu^+\bar{\nu}$, predicts an equal number of $\nu N \rightarrow e^-e^-X$ events; no such events have been reported¹³ so we infer that this is not an important source of μ^+e^- . Figure 5 shows LH models: similar arguments exclude E^0 cascades in LC models.

(v) In LC models with $\nu d \rightarrow M^+t$ new quark production, the semileptonic decay $t \rightarrow d\mu^+\nu$ gives an extra μ^+ which does not help in explaining $\mu^+\mu^+\mu^+$ events.

Antineutrino production of trileptons and dileptons can also be used to discriminate between LC and

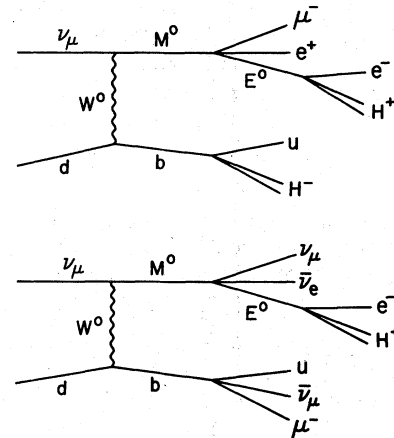


FIG. 5. Diagrams with $M^0 \rightarrow E^0$ decays in LH models that we argue are unimportant for $\nu N \rightarrow \mu^+e^-X$. Analogous diagrams exist in LC models, and are similarly unimportant.

LH models. Straightforward analogs of the diagrams in Figs. 1 and 2 predict substantial rates for $\bar{\nu} \rightarrow 3\mu$, $\bar{\nu} \rightarrow 2\mu$, $\bar{\nu} \rightarrow \mu e$, etc. In any of the models with incident antineutrinos, all particles coming from the lepton vertex are charge conjugated with respect to the neutrino case. At the hadron vertex the transitions $d \rightarrow u$, $d \rightarrow t$, and $d \rightarrow b$ for neutrino scattering are replaced by $u \rightarrow d$, $u \rightarrow b$, and $d \rightarrow b$, respectively, for antineutrino scattering (the V, A nature of the quark coupling may also change, depending on the model). In some models¹⁰ the quark coupling for antineutrinos may not exist, although the corresponding coupling for a neutrino does. For allowed antineutrino trimuon production, the muon charges are quite different in LC and LH models, namely

$$\begin{aligned} \bar{\nu} N \rightarrow \mu^+\mu^+\mu^+X, & \text{ for LC models} \\ \bar{\nu} N \rightarrow \mu^+\mu^-\mu^+X, & \text{ for LH models,} \end{aligned} \quad (6)$$

This is simply because LH models involve neutral currents, and hence the leptons from the hadron vertex have the same charge in both ν and $\bar{\nu}$ cases, whereas all leptons from the lepton vertex are charge conjugated. Thus the charge topology of antineutrino trimuons can distinguish very simply between LC and LH diagrams, both of which yield the same topology $\nu \rightarrow \mu^+\mu^-\mu^+$ for neutrino trimuons.

Similarly, the antineutrino analogs of the diagrams in Fig. 2 lead to quite different dilepton processes, namely:

$$\begin{aligned} \bar{\nu} N \rightarrow \mu^+e^+X \text{ or } \mu^+\mu^+X, & \text{ for LC models} \\ \bar{\nu} N \rightarrow \mu^+e^-X \text{ or } \mu^+\mu^-X, & \text{ for LH models.} \end{aligned} \quad (7)$$

Other LC diagrams with $M^+ \rightarrow \bar{M}^0H^+$, $\bar{M}^0 \rightarrow \mu^+\bar{l}^-$ give $\bar{\nu} \rightarrow \mu^+\bar{l}^-$ events; also such events occur through charm production and decay. But LH diagrams

cannot give $\bar{\nu} \rightarrow \mu^+ e^+$ nor $\bar{\nu} \rightarrow \mu^+ \mu^+$ events; such events cannot occur through simple charm production and decay (assuming charm conserving neutral currents), so the presence or absence of such

events can distinguish between LC and LH mechanisms.

We thank D. Reeder for discussions.

*Work supported in part by the University of Wisconsin Research Committee with funds granted by the Wisconsin Alumni Research Foundation, and in part by the U. S. Energy Research and Development Administration under Contract No. E(11-1)-881, COO-602.

†On leave from Rutherford Laboratory, Chilton, Didcot, Oxon, England.

¹A. Benvenuti *et al.*, Phys. Rev. Lett. **38**, 1110 (1977); **38**, 1183 (1977).

²B. C. Barish *et al.*, Phys. Rev. Lett. **38**, 577 (1977).

³V. Barger *et al.*, Phys. Rev. Lett. **38**, 1190 (1977); Phys. Rev. D **16**, 2141 (1977); Univ. of Wisconsin—Madison Report No. COO-597, 1977 (unpublished); Phys. Rev. D **16**, 3170 (1977).

⁴C. Albright, J. Smith, and J. A. M. Vermaseren, Phys. Rev. Lett. **38**, 1187 (1977); Phys. Rev. D **16**, 3182 (1977).

⁵P. Langacker and G. Segrè, Phys. Rev. Lett. **39**, 259 (1977) and Pennsylvania Report No. UPR-0073T, 1977 (unpublished).

⁶B. W. Lee and S. Weinberg, Phys. Rev. Lett. **38**, 1237 (1977).

⁷A. Zee, F. Wilczek, and S. B. Treiman, Phys. Lett. **68B**, 369 (1977).

⁸R. M. Barnett and L. N. Chang, SLAC Report No. SLAC-PUB 1932 (unpublished).

⁹E. L. Lipmanov, Zh. Eksp. Teor. Fiz. Pis'ma Red. **23**, 363 (1976) [JETP Lett. **23**, 327 (1976)].

¹⁰D. Horn and G. G. Ross, Phys. Lett. **69B**, 364 (1977).

¹¹After completion of this paper, we received a report from C. H. Albright, J. Smith, and J. A. M. Vermaseren [Phys. Rev. D **16**, 3204 (1977)] that also discusses electron signals from heavy-lepton cascades.

¹²A. Benvenuti *et al.*, Phys. Rev. Lett. **35**, 1199 (1975); D. Cline, in *Particles and Fields '76*, proceedings of the Annual Meeting of the Division of Particles and Fields of the APS, Brookhaven National Laboratory, edited by H. Gordon and R. F. Peierls (BNL, Upton, New York, 1977), p. D37.

¹³C. Baltay, CERN seminar, 1977 (unpublished).

¹⁴V. Barger, T. Gottschalk, and R. J. N. Phillips, Phys. Lett. **70B**, 51 (1977).

¹⁵R. Odorico, CERN Report No. TH-2360, 1977 (unpublished).

¹⁶M. Holder *et al.*, Phys. Lett. **69B**, 377 (1977).

¹⁷V. Barger *et al.*, Univ. of Wisconsin—Madison Report No. COO-600, 1977 (unpublished).

¹⁸A. Soni, Phys. Rev. D **9**, 2092 (1975); **11**, 624 (1975); C. H. Albright, *ibid.* **12**, 1319 (1975); **13**, 2508 (1976); L. N. Chang, E. Derman, and J. N. Ng, *ibid.* **12**, 3539 (1975).